Motor control processes moderate visual working memory gating

Şahcan Özdemir[1], Eren Günseli[2] & Daniel Schneider[1]

1. Leibniz Research Centre for Working Environment and Human Factors, Dortmund, Germany
2. Department of Psychology, Sabancı University, Istanbul, Turkey

Corresponding Author

Şahcan Özdemir (oezdemir@ifado.de)

Data Availability

All data and materials are shared publicly on Open Science Framework (https://osf.io/7fve8/). Only anonymized data are shared.

Code Availability

All scripts related to data analysis and experimental setup are shared publicly on Open Science Framework (https://osf.io/7fve8/).

Author Contributions

All authors contributed to the conceptualization of this study. Ş.Ö. and D.S. designed the experiment. Ş.Ö. collected the data. Ş.Ö. and D.S. conducted the data analysis. All authors discussed the interpretation of the results and wrote the manuscript.

Competing Interests

The authors declare no competing interests.

Keywords

working memory, action planning, gating, interference

ABSTRACT

Gating processes that regulate sensory input into visual working memory (WM) and the execution of planned actions share neural mechanisms, suggesting a mutual interaction. In a preregistered study (OSF), we examined how this interaction may result in sensory interference during WM storage using a delayed-match-to-sample task. Participants memorized the color of a target stimulus for later report on a color wheel. The shape of the target indicated which hand they would adjust the color wheel with. During the retention interval, an interference task was presented, requiring a response with either the same or different hand as the main task. In half of the interference trials, the interfering task cue was also colored to introduce visual interference. EEG results showed early motor planning during sensory encoding, evidenced by mu/beta suppression contralateral to the responding hand. The interference task only impaired WM performance when it included an irrelevant color, indicating that the interference effect was primarily driven by the irrelevant sensory information. In addition, color reporting in the WM task was biased toward the irrelevant color. This was more pronounced when both tasks were performed with the same hand, suggesting a selective gating mechanism dependent on motor control processes. This effect was mitigated by a control mechanism, which was evident in frontal theta activity, where higher power predicted lower bias on the single-trial level. Our findings thus reveal that sensory WM updating can be induced by interfering motor actions, which can be compensated by a reactive control mechanism.

SIGNIFICANCE STATEMENT

Working memory is increasingly recognized not only as a system for maintaining sensory representations of the past, but also as one that creates prospective representations serving future actions. This shift in perspective raises fundamental questions about how motor planning shapes the way information enters and is maintained in working memory. Our study demonstrates a novel interaction between motor processes and working memory: When a stored memory representation is linked to a specific motor response, it becomes particularly vulnerable to interference from sensory information requiring the same motor response. Using EEG recordings, we identify neural signatures of this interaction and reveal a frontal control mechanism that can counteract the influence of irrelevant mental representations on working memory. These findings provide important insights into the fundamental architecture of memory, showing for the first time that motor processes not only guide the use of stored information but also influence how new information is integrated into working memory representations.

INTRODUCTION

Working memory (WM) serves a critical function in human cognition by maintaining and manipulating task-relevant information (Baddeley, 2003). Recent research has increasingly focused on the 'task-relevant' aspect of WM, emphasizing its prospective nature – i.e., how flexibly WM adapts to task requirements (Gunseli et al., 2014; Huang, 2015; for reviews see Miller et al., 2018; Olivers & Roelfsema, 2020; Postle, 2006; van Ede, 2020; Van Ede & Nobre, 2023). The shift towards a prospective view has expanded the examination of how sensory representations are maintained and manipulated in a bidirectional relationship with prospective action representations (Boettcher et al., 2021; Nasrawi et al., 2023; Olivers & Roelfsema, 2020; Rösner et al., 2022; Sahakian et al., 2025; Schneider et al., 2017; Trentin et al., 2023). Building on this framework, the present study investigates the influence of action planning on WM gating processes, specifically examining the extent to which the storage of relevant information in WM is susceptible to interfering stimuli.

Building on the prospective aspect of WM, recent studies have highlighted the relationship between sensory and motor representations (Heuer et al., 2020; Nasrawi et al., 2023; Rösner et al., 2022; Trentin et al., 2023, 2024). This interaction involves the preparation of a motor plan for a WM item that is anticipated to be reported (Boettcher et al., 2021; Nasrawi et al., 2023; Rösner et al., 2022; Schneider et al., 2017; van Ede et al., 2019). In this context, evidence for motor preparation is characterized by the suppression of mu/beta oscillatory power (8-14/14-30 Hz, respectively) over the sensorimotor cortex contralateral to the responding hand, which can occur concurrently with the attentional selection of the target item, indexed by an alpha-band (8-12 Hz) power suppression over posterior/occipital electrodes contralateral to its location (Günseli et al., 2019; Woodman et al., 2022). Action preparation also leads to the prioritization of action-relevant features of the WM representation. For example, Heuer et al. (2020) demonstrated that when participants maintain stimuli of various sizes and colors, subsequent action cues specifying a response affect which memory feature is prioritized. Specifically, preparing to grasp the item prioritized the item's size while preparing to point at it prioritized its color. The planning of motor actions also influences interference among objects stored in WM. Trentin et al. (2024) demonstrated that the repulsion bias between two WM items was greater when they were associated with different future actions than when they shared the same action plan.

These findings collectively demonstrate that motor planning significantly shapes how information is represented and prioritized within WM. However, an important question remains: If motor processes influence how information is stored in WM, might they also regulate how new information enters WM during ongoing storage? Such a relationship is plausible, given evidence of overlapping neural mechanisms between motor control processes and WM input gating, i.e., the regulation of information flow into WM (Chatham & Badre, 2015). Therefore, the planning or execution of a motor response might indirectly influence WM's susceptibility to new information, either enhancing (open gate) or reducing (closed gate) information uptake. Our investigation specifically examines how this input gating process is modulated by correspondence between motor representations maintained in WM and motor responses executed during an interfering task. We hypothesize that sensory inputs associated with corresponding motor responses are more likely to gain access to WM, suggesting a selective gating mechanism that prioritizes information aligned with stored motor plans.

To test this hypothesis, we employed a delayed match-to-sample WM task that required reporting the color of a target stimulus. We manipulated motor planning by assigning the shape of the target object to indicate the use of either the left or right hand for color report. Additionally, we introduced an interference task during the WM storage interval, requiring participants to perform a secondary action with either the same or a different hand as used in the primary task. In half of the trials, the cue during this secondary task was colored. This color was irrelevant to either task, allowing us to assess the handling of sensory distractors during WM storage.

Our study was guided by three preregistered hypotheses (OSF). Hypothesis 1 proposed that motor plans would be stored in WM early in the retention interval, which would be evident in contralateral suppression of oscillatory power in the mu and beta frequency ranges (~8-30 Hz) prior to the presentation of the interfering task (Boettcher et al., 2021; Nasrawi et al., 2023; Rösner et al., 2022; Schneider et al., 2017; van Ede et al., 2019; Zickerick et al., 2021). Moreover, Hypothesis 1 also predicted that this mu and beta power lateralization would correlate with the accuracy of later color report (Boettcher et al., 2021; Nasrawi et al., 2023). Although we observed oscillatory correlates of motor planning early during encoding, there was no relation to later retrieval performance. Hypothesis II predicted larger error in the visuomotor interference (colored interference task cue) than the motor interference condition (non-colored interference task cue) (Lorenc et al., 2021, 2021; Rademaker et al., 2015; Saito

et al., 2023). Results confirmed higher error rates after visuomotor interference, with no difference between baseline (no interference) and motor interference conditions, indicating that the irrelevant color interfered with later report from WM. Lastly, Hypothesis III predicted that interfering sensory input would gain preferential access to WM when there is a correspondence of motor plans stored in WM and responses to the interference task. Our results supported this, showing a higher attraction bias towards the irrelevant color when the same hand was used for both tasks. This effect was accompanied by an increase in frontal theta power following the response to the secondary task, potentially reflecting a reactive control mechanism to reduce the impact of task-irrelevant information on WM (Rac-Lubashevsky & Kessler, 2015, 2018).

METHODS

Participants

A total of 32 (M_{age}= 23.71; SD_{age} = 2.93; 20 Female) participants participated in the experiment, and were compensated with either money (12€ per hour) or course credits. Two participants were excluded from further analysis due to their misunderstanding of the instructions (i.e., pressing the response buttons already during target presentation), and one participant was excluded based on the exclusion criteria detailed below. Additionally, one participant's data was used only for the behavioral analysis due to excessive noise in the EEG signal. Thus, the final behavioral analysis included 29 participants while the EEG analyses were conducted with 28 participants.

We calculated the target number of participants using G*Power software (Faul et al., 2007). A priori sample size calculations were conducted for a one-tailed paired-samples t-test referring to the response correspondence effect on attraction bias (Hypothesis III; see Behavioral Analysis section). These calculations employed an alpha level of .05 to control for Type I error, with a desired power of 95%. Given the novelty of the effect under investigation and the lack of directly comparable studies, we used the effect size (Cohen's d = 0.71) from a study on active vs. passive engagement with a distractor during working memory storage as a reference (Saito et al., 2023). This analysis yielded 23 as the minimum number of participants to achieve the desired statistical power. Since this study did not align perfectly with our research questions, the target number of participants has been increased slightly to account for a potentially weaker effect.

To further ensure the robustness of our sample size, we reviewed studies measuring mu/beta suppression during motor planning in a WM experiment, where three studies used a sample size of 24-26 (Boettcher et al., 2021; Rösner et al., 2022; van Ede et al., 2019). To accommodate the counterbalancing of the assignment of stimulus shape to responding hand (see Procedure), we determined an even number of 26 participants as the target sample (see OSF preregistration). Our final data collection slightly exceeded this target by two datasets (i.e., 28 datasets including EEG data) due to inaccurate coordination with the laboratory staff. Importantly, conducting the analyses only with the first 26 usable datasets did not alter the result patterns.

Data quality is assured by the preregistered exclusion criteria. Participants with an accuracy lower than 70% in using the correct hand in the main task were excluded from further analyses. Furthermore, participants whose mean absolute error was more than 2 standard deviations away from the sample mean were discarded. As indicated above, this led to the rejection of one dataset from all further analyses.

Ethics statement

This study was conducted under the ethics approval of the local ethics committee at the Leibniz Research Centre for Working Environment and Human Factors and in accordance with the Declaration of Helsinki.

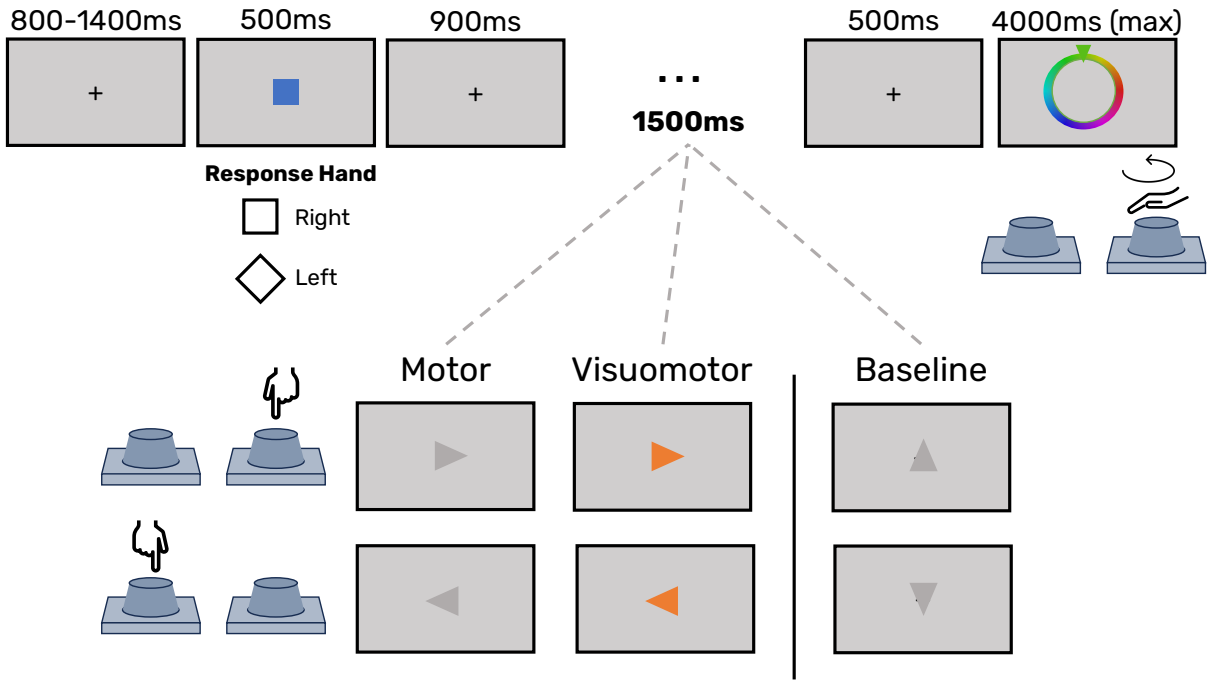

Figure 1. Illustration of the experimental procedure. Participants completed a delayed match-to-sample task, and the response hand was manipulated. The color of the target had to be remembered for later report, while its shape indicated which hand to use for that. Color report was done by adjusting a color wheel to display the target color through rotating one of two response knobs. During the maintenance phase, participants performed an interference task requiring a response to the direction of a central cue (pressing the left vs. right knob) that either corresponded or did not correspond to the hand used in the main task. In half of the interference trials, the interference cue was colored, introducing visual interference. In the baseline condition (cue pointing up or down), there was no response required during maintenance.

Apparatus, stimuli, and procedure

The experiment was conducted using a ViSaGe MKII Stimulus Generator (Cambridge Research Systems, Rochester, UK) and presented on a 22-inch CRT screen (resolution: 1024x768, refresh rate: 100 Hz) in a dimly lit, electrically shielded experiment room. The paradigm was prepared and coded on Lazarus IDE with free Pascal. Responses were collected via two response knobs. These knobs were constructed from 3D-printed material, covering two rotary encoders attached to an Arduino processor (Arduino, Lombardia, Italy). The knobs could be rotated continuously, and the rotational data were decoded by the two rotary encoders and transmitted to the experimental setup using Arduino. The experiment consisted of 1200 trials in 10 blocks. There was a short break of ~2 minutes between the blocks and a longer break of ~5-10 minutes halfway through the experiment.

For stimulus presentation, 180 colors were sampled from HSV color space. The saturation and the value were kept constant (S=.85, V=.9). According to the gradual change in hue (from 1 to 360, 2 degrees per step), 180 colors were sampled at equal distances. Each sample color was used as the target color 6 to 7 times. The sampled 180 colors were then placed on a visual circle to prepare a color wheel (the probe) in each trial. The orientation of the color wheel was randomized to prevent a re-coding of color into a spatial location on the color wheel.

Before the experiment, all participants completed a handedness questionnaire (Oldfield, 1971) to assess their dominant hand. All participants were classified as right-handed. Due to the nature of the experimental task, their color vision was evaluated via the Ishihara Test for Color Blindness.

Participants were asked to complete a delayed match-to-sample WM task in each trial. First, they were shown a target item centered on the screen to remember its color until the end of the trial. The target was presented as either a square or a diamond shape (1.83° x 1.83°) at the center of the screen. The shape of the target item informed participants whether to use their right or left hand for color report (e.g., right hand for square, left hand for diamond). Shape-hand assignment was counterbalanced across participants. The target presentation was followed by a fixation cross (0.44° x 0.44°) for 900ms. Then, participants were presented with the interference period for 1500ms. What participants encountered in the interference period differed across three conditions: motor interference, visuomotor interference, and baseline.

In the motor interference condition (400 trials), we presented a gray arrow as a cue which either pointed to right or left (HSV: 0, 0, 0.5; side length: 1.83°). Participants were instructed to click the response knob on the side the arrow pointed to as quickly as possible. In the visuomotor interference condition (400 trials) participants were instructed to do the same task, but this time the cue color varied. The cue color was 60-90 degrees away from the target color on the color wheel. Thus, the color of the cue added a visual interference aspect to this condition. In the baseline condition (400 trials), participants were shown a gray arrow which pointed either upwards or downwards. In this condition, they were expected to ignore the arrow and respond only to the presentation of the later memory probe.

Following this interference period, participants were presented with another fixation cross for 500ms. Then they were instructed to indicate the memorized color on a color wheel (diameter:

5°; thickness: 1°) by rotating the response knob which had been indicated by the shape of the target item at the beginning of the trial. By rotating the knob, participants moved a small arrow over the color wheel to select the desired color. The color of the arrow (or cursor) dynamically updated as it moved along the wheel, matching the currently selected color to facilitate accurate selection. To finalize their response, participants were required to press the knob after having completed their color adjustment. Each trial allowed participants a maximum of three seconds to complete their response. If the participant did not press the knob within this time frame, the last color indicated by the cursor was automatically recorded as the given response.

Behavioral Analyses

Registered analysis

Only trials in which participants responded to both the main task and the interference task using the cued hand were included in the behavioral analysis. In each trial, the absolute difference between the given response and the target color was calculated as an error (relative to their position on the color wheel).

For all behavioral analyses, we provide both frequentist and Bayesian statistics. In Bayesian repeated measures ANOVAs, the BF_{10} value represents the comparison of the tested model (with a given main effect) against the null model. When analyzing interactions, the null model includes the main effects (Bergh et al., 2020).

For Hypothesis II (see above), absolute errors were averaged for each condition to reveal the magnitude of the interference effect. We expected to see more interference when the interfering task had an irrelevant visual feature (visuomotor condition), compared to the motor interference condition. To test the difference between different types of interference and their relation to the baseline condition, we conducted a one-way ANOVA with three levels (visuomotor interference, motor interference, baseline). All p-values from the multiple comparisons following the ANOVA were Holm adjusted.

Hypothesis III focused on how the WM representation is biased by the interfering visual object in the visuomotor interference condition. To examine this effect, we calculated the attraction bias. Since the effect is calculated relative to the interference color, this could only be realized in the visuomotor interference condition. In each trial, an attraction bias was assumed if the reported color lay in the direction of the interference color on the color wheel. The opposite

case is considered a repulsion bias (Chunharas et al., 2022). For analyzing this bias, each error value between the actual and the reported color was assigned a positive or a negative value, depending on whether there was a shift in the direction of or against the position of the interference color. Then, we calculated the average of assigned errors for each condition to determine the bias terms for each participant. We expected to observe a stronger attraction bias when the main and secondary tasks were executed with the same hand (corresponding condition) than with different hands (non-corresponding condition). Therefore, we conducted a one-tailed paired-samples t-test between the bias of the compatible and incompatible visuomotor interference conditions. Final statistical tests of behavioral analyses were conducted in JASP (Love et al., 2019), after transferring processed data from MATLAB, unless stated otherwise.

Exploratory analysis

To assess the effect of different types of interference on WM representations, we compared the precision across conditions for each participant. For this analysis, errors were signed as positive if they were clockwise from the target color, and negative if they were counterclockwise. We then calculated the standard deviation (SD) of the signed errors for each condition separately for each participant and defined precision as 1/SD. As in Hypothesis II, we conducted a one-way repeated measures ANOVA with three levels (visuomotor interference, motor interference, baseline).

Furthermore, we compared response times (RT) and accuracies in the interference task. We aimed to investigate whether differences in hand correspondence conditions were related to task difficulty or complexity. Our assumption was that if no such differences existed, there would be no variation in RTs or accuracies between the corresponding and non-corresponding conditions. We compared both RTs and accuracies using a 2x2 one-way ANOVA (motor/visuomotor interference, corresponding/non-corresponding response hand).

EEG recording, preprocessing and analyses

Recording

EEG was recorded with 64 Ag/AgCI passive electrodes (Easycap Gmbh, Herrsching, Germany) with a sampling rate of 1000 Hz. NeurOne Tesla AC amplifiers (Bittium Biosignals Ltd, Kuopio, Finland) were used for data collection with a 250 Hz low-pass filter. We used the FCz channel as the reference and AFz as the ground electrode position.

Preprocessing

We used MATLAB (R2023b, Mathworks, Natick, USA), the ERPLAB toolbox (Lopez-Calderon & Luck, 2014), and the EEGLAB toolbox (Delorme & Makeig, 2004) for the analysis of the EEG data. First, a high-pass filter with a 0.1 Hz threshold and a low-pass filter with a 40 Hz threshold were applied using an IIR Butterworth filter via the ERPLAB Toolbox's *pop_basicfilter* (default order: 3*(sampling rate/low cut off)) function. After filtering, channels with dense artifacts were rejected using the *pop_rejchan* function (kurtosis threshold: 15), an automated process provided by EEGLAB. Frontal electrodes were excluded from this rejection procedure to maximize the capture of eye-related variance in the subsequent independent component analysis (ICA). Following channel rejection, the data were re-referenced by setting the average of all channels as the new reference. The steps between re-referencing and ICA were performed only as preparation for ICA. After calculating the IC weights, the pipeline reverted to the re-referencing stage, where the IC weights were applied to the re-referenced data, disregarding the intermediate steps.

After re-referencing, the data were downsampled to 200 Hz and high-pass filtered with a 1 Hz threshold using a Hamming-windowed sinc FIR filter (*pop_eegfiltnew,* filter order: 661, transition bandwidth: 1 Hz, cutoff frequency at −6 dB: 0.5 Hz). The data were then epoched, starting 1000ms before stimulus onset and ending 4400ms after stimulus onset. A baseline correction was applied using the 200ms period prior to stimulus onset. Automated trial rejection was then performed using EEGLAB's *pop_autorej* function (threshold: 500 µV, maximum percentage of rejected trials per iteration: 5). ICA was applied following trial rejection.

Independent components (ICs) were then identified using the ICLabel classifier for EEGLAB, classifying components into categories such as brain, muscle, eye movements, heart activity, channel noise, line noise, and "other" (Pion-Tonachini et al., 2019). ICs with a probability of being eye movement greater than 30%, and with a probability of being brain signal less than 10%, were marked for later rejection.

After IC rejection, the remaining IC information was attached back to the re-referenced data, bypassing the ICA preparation stages. The data were then epoched from -1000ms to 4400ms, time point zero being the onset of the target stimulus. A baseline correction was applied using the 200ms pre-stimulus time window. IC components labeled as artifacts were removed. Any remaining noisy trials were rejected using the same automated trial rejection method applied

during the ICA preparation stages. Finally, missing channels were interpolated using the *pop_interp* function in EEGLAB, with spherical spline interpolation, and the data were downsampled to 250 Hz.

Our preprocessing pipeline resulted in 31.32 ICs (SD = 7.78), 933.32 trials (SD = 151.51), and 63.32 channels (SD = 1.38) remaining on average.

Time-frequency decomposition

We first calculated the time-frequency decomposition of the data. For each trial and channel, the oscillatory power for each frequency was calculated from 4 to 30 Hz on a logarithmic scale in 26 steps. For each frequency in the given spectrum, a complex Morlet wavelet was created by tapering a sinusoid (ei2ft) of the given frequency with a Gaussian [(e-t2/2s2; s is the width of the Gaussian; s = /(2f) corresponds to the number of cycles of wavelet)]. Our zero padded data, and the Morlet wavelets were Fast Fourier transformed (FFT). Convolution in TF decomposition was done by multiplying the signal's Fast Fourier transform with the Fast Fourier transform of a complex Morlet wavelet in each frequency by taking the dot product. Then an inverse Fast Fourier transform was applied to get the time-domain result. We applied a baseline normalization by averaging the -400ms to -100ms time interval in all trials and divided each trial by this averaged value and converted the measurement to decibel (dB).

Registered analysis

To explore the first part of Hypothesis I, which predicts motor planning during the visual encoding of to-be-memorized colors, we calculated contralateral mu/beta suppression following target presentation. This refers to the suppression of ~8-30 Hz activity on the side opposite to the hand being used for a response in the main task, measured over the centro-parietal EEG channels (C3, C4, CP3, CP4) (Rösner et al., 2022). Previous research has established the contralateral mu and beta suppression as a signature of action planning (Boettcher et al., 2021; Nasrawi et al., 2023; Rösner et al., 2022; Schneider et al., 2017; van Ede et al., 2019).

First, we calculated both contralateral and ipsilateral power across all time points and frequencies by assigning channels regarding their position to the main task response hand. Contralateral power was always derived from the channels on the side opposite to the responding hand for the main task in each trial. This analysis focused on the encoding stage,

defined as the period from 0ms (target stimulus onset) to 1400ms (interference cue onset). Since no experimental conditions could have had an influence on EEG response in this time interval, we averaged all trials across conditions for each participant. Lateralization in oscillatory power was calculated as the contralateral-minus-ipsilateral difference. To determine whether there was significantly stronger suppression on the contralateral side, we performed a cluster-based permutation test. This procedure began by comparing contralateral minus ipsilateral oscillatory power to zero using a one-sample t-test at each time and frequency point, identifying significant points where $p < .05$. We then randomly assigned the sign (positive or negative) of the difference for each participant's data points across 10,000 permutations, creating a distribution of permuted significant cluster sizes. Clusters from the original data that were larger than the 95th percentile of the permuted clusters were considered significant. For the significant cluster, we calculated Cohen's d for each datapoint and reported the maximum and average effect size for the cluster.

Hypothesis I also predicts that greater contralateral mu/beta suppression during the encoding stage will be associated with higher WM accuracy (Boettcher et al., 2021; Nasrawi et al., 2023). To test this hypothesis, we used a median split approach for each condition separately. First, we calculated the median error value (based on absolute errors) for each participant. Then, for each condition, we calculated the average contralateral mu suppression for trials where the error was below the median and for trials where the error was above the median. To determine whether there was a significant difference in contralateral mu/beta suppression between the below-median and above-median trials, we applied the same cluster-based permutation test procedure explained above. This test compared the two performance conditions over time (0-1400ms), conducted separately for each experimental condition. The aim was to identify any time-frequency clusters where a persistent and significant difference in contralateral suppression occurred between the below- and above-median trials.

Exploratory Analysis

While the prior analyses address motor planning processes during the encoding of visual information in WM, we also investigated to which extent the presentation of an irrelevant color affected the re-focusing on primary task information after completion of the secondary task. Prior investigations have revealed that this process can be tracked by the suppression of oscillatory power in the alpha frequency range at posterior electrodes (Woodman et al., 2022). Therefore, posterior oscillatory power was calculated as the average oscillatory power at the

Oz, O1, O2, Pz, PO3, and PO4 channels. For the between-condition comparison, we applied a cluster-based permutation test as explained above. The two interference conditions (motor, visuomotor) were compared against the baseline condition and against each other during the interference interval (1400-3400ms after target presentation; see Figure 3B). We did not average over the alpha band (8-12 Hz) to see the distribution of the effect across frequencies more clearly; however, we expected the effect to be centered around alpha.

Given that the analysis of posterior oscillatory power showed differences between the visuomotor and motor interference conditions (see Figure 3B), we aimed to examine the time course of this difference concerning the secondary task response. This approach allowed us to determine whether the onset of the difference aligned with the secondary task response, which would prove that it is rather about the refocusing on the visual content from the primary WM task than about the visual processing of the secondary task cues. To achieve this, we calculated the oscillatory power time-locked to the response to the secondary task. After the regular time-frequency decomposition, we adjusted the timeline of each trial to be centered around the response to the secondary task. Similar to the analyses of posterior oscillatory power time-locked to secondary task cue onset, we calculated the average over trials for each condition and each subject. We then performed the same comparisons as with the stimulus-onset-locked posterior alpha analysis from 700ms prior to 700ms after the response (Figure 3C; not including the baseline condition since there was no secondary task response).

In the above analyses, we conducted all examinations using pre-selected channels as regions of interest to investigate specific attentional and motor planning mechanisms. However, none of these analyses directly addressed the EEG correlates as a function of Hypothesis III (see Results), where we demonstrate the effect of hand correspondence on WM gating. Therefore, we further compared the corresponding and non-corresponding visuomotor conditions in an exploratory manner. First, we averaged the time-frequency decomposition for each condition for every participant, and we conducted another cluster-based permutation test including all channels, all frequency bands and the time interval following interference presentation (1400-3400ms) across participants. To be able to explore the differences over all channels, we used the FieldTrip (Oostenveld et al., 2011) cluster-based permutation test protocol. For the acquisition of the statistics, the *ft_freqstatistics* function was used (estimation method: Monte-Carlo, cluster correction, alpha: .05, t-statistics, cluster formation approach: t-sum (default), minimum number of channels for cluster formation: 2, false alarm rate: .05, number of

randomizations 5000). For the calculation of neighboring channels, distances between channels were determined by the automated FieldTrip procedure. Due to the t-sum approach used in the procedure, t-values were summed for each cluster, and clusters from each permutation were distributed according to their t-sum values. The actual clusters with a t-sum higher than 95 percent of permuted clusters was considered significant.

To achieve a meaningful distribution of channel contributions to the observed effects, a procedure from Ülkü et al. (2024) was adapted. The number of significant data points from each channel was divided by the number from the channel with the highest number of significant data points, creating a value representing the relative contribution of each channel. Channels scoring more than 0.7 were considered part of the identified cluster. Significant clusters in the time-frequency domain were displayed in a contour map, along with the contributing channels.

Our exploratory analysis revealed a frontal theta difference between the corresponding and non-corresponding visuomotor interference conditions at the end of the interference cue presentation window (see Results). Further, we aimed to explore whether this TF pattern correlates with the strength of the attraction bias on a trial-by-trial basis. To calculate this, we conducted a correlation test, computing Pearson's correlation coefficient between each time-frequency power point and the attraction bias across all trials. We then applied Fisher's z-transformation, which involves calculating the inverse hyperbolic tangent of the coefficient distribution. This produced a matrix of time points x frequencies for each subject, each channel, and each condition (only sub-conditions of the visuomotor interference condition) with Fisher z values. We then averaged the frontal channels AF3, AF4, F1, F3 and F5 which were provided by the previous analysis as the biggest contributors of the theta effect observed (Figure 4C) and conducted a cluster-based permutation test against zero for both conditions.

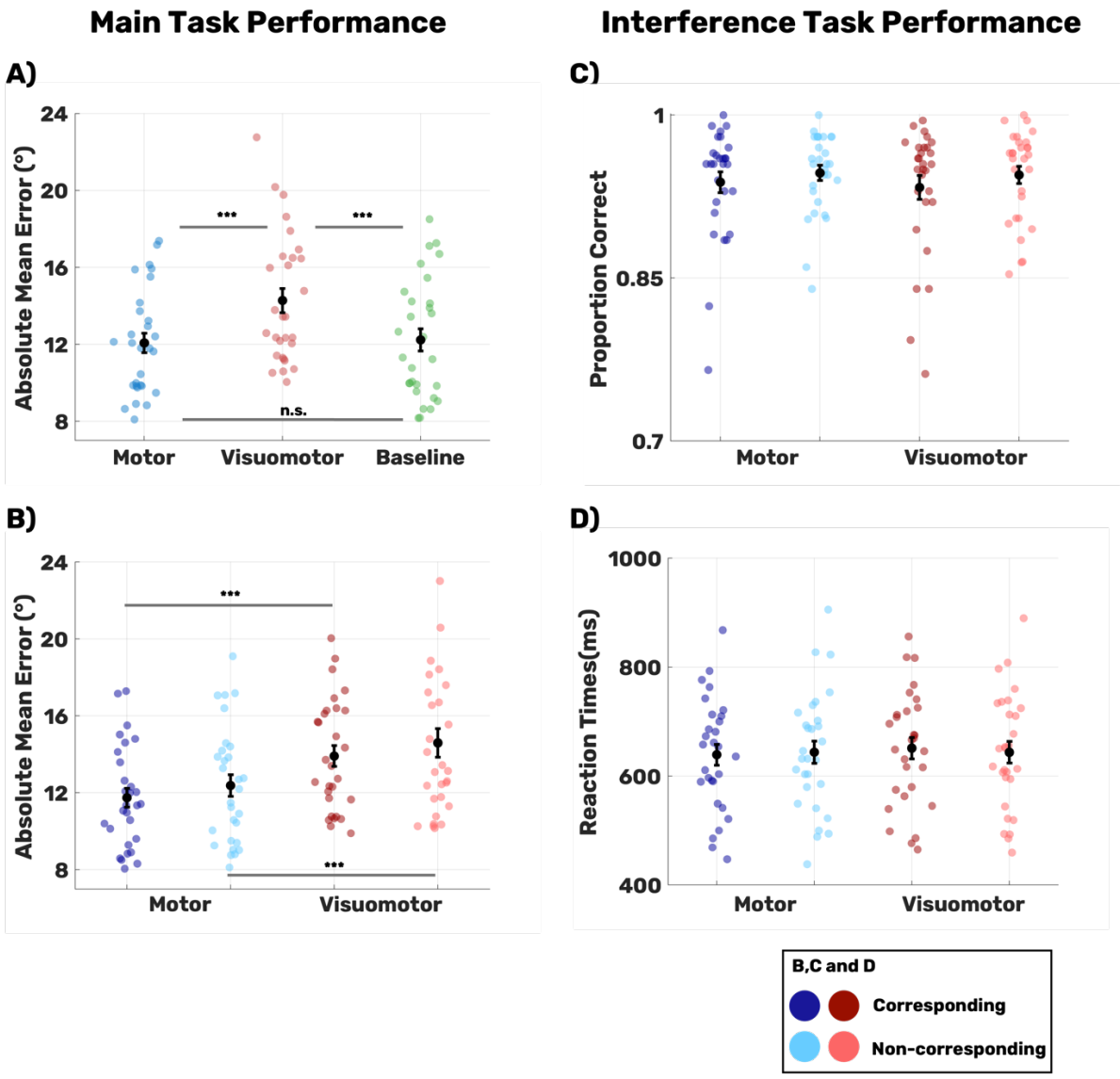

Figure 2. Illustration of Behavioral Performance. (*p<.05, **p<.01, ***p<.001) . **A–B)** These panels compare absolute mean errors in the main task. **A)** The highest error rates occurred in the visuomotor interference condition, while motor interference did not differ from baseline. **B)** Hand manipulation had a marginal effect on main task performance. Errors were slightly higher in the non-corresponding interference condition. However, post hoc comparisons within motor or visuomotor conditions revealed no significant differences. As expected, visuomotor interference had the strongest impact on performance. **C–D)** There were no significant differences between conditions in interference task performance. Both correct hand usage and reaction times (RTs) remained consistent across conditions.

RESULTS

Behavioral results

Effects of interference on accuracy

We conducted a repeated measures ANOVA with three levels of interference type (motor interference, visuomotor interference, baseline) to determine whether adding a visual feature (the color of the interference task cue) interferes with the main task WM representation

(Hypothesis II). We analyzed absolute average errors across conditions for each participant. Results indicated a main effect of interference type, $F(2, 56) = 35.35$, $p < .001$, $\eta^2 = .558$, $BF_{10}=5.48x10^8$. Post hoc comparisons revealed that visuomotor interference led to significantly higher errors compared to both the motor interference ($t(28) = 7.551$, $p < .001$, d = 0.718, 95% CI [2.933 1.488], $BF_{10}=6.24x10^5$) and the baseline condition ($t(28) = 6.981$, $p_{holm} < .001$, d = 0.664, 95% CI [2.766 6.981], $BF_{10}=1.51x10^4$). No significant difference was found between the motor interference and the baseline condition ($t(28) =0.570$, $p_{holm} = .571$, d = 0.054, 95% CI [0.889 -0.556], $BF_{10}=0.24$).

We also examined the effect of corresponding vs. non-corresponding motor features between the main task and the interference task on behavioral performance to observe if shared motor features affect the handling of secondary tasks during WM storage. For this analysis, we used two factors: interference type (motor, visuomotor) and whether the response hands were corresponding or non-corresponding between tasks. To achieve this, we conducted a 2x2 repeated-measures ANOVA. Results showed a main effect of interference type (as it was shown in the previous analysis, $F(1,28) = 59.831$, $p < .001$, $\eta^2 = .447$, $BF_{10}=7.23x10^5$) and a main effect of response-hand correspondence ($F(1,28) = 5.371$, $p =.028$, $\eta^2 = .04$, $BF_{10}=2.18$), with no significant interaction ($F(1,28) = 0.018$, $p =.895$, $\eta^2 = 5.87x10^{-6}$, $BF_{10}=0.33$). Post hoc testing indicated that when the hands used for the tasks were non-corresponding, WM accuracy was lower ($t(28) = 2.137$, $p_{holm} = .028$, d= 0.207, %95 CI [0.077 1.244], $BF_{10}=4.4$). This shows the effect of an interrupting task was slightly stronger when the two responding hands did not correspond between tasks.

Effects of interference on precision

We conducted a similar analysis on WM precision (1/SD; see methods section). The comparisons of precision yielded results consistent with those of accuracy, revealing a main effect of interference type ($F(2, 56) = 12.915$, $p < .001$, $\eta^2 = 0.316$, $BF_{10}=769.9$). Specifically, precision was lower in the visuomotor interference condition than the motor interference ($t(28) = 4.54$, $p_{holm} < .001$, d = 0.573, 95% CI [0.204 0.942], $BF_{10}=1803.5$). However, precision in the motor interference condition did not differ from the baseline condition ($t(28) = 0.299$, $p_{holm} =.76$, d = 0.038, 95% CI [-0.278 0.354], $BF_{10}=0.205$).

Next, we examined the effect of hand correspondence in relation to the interference type. The analysis demonstrated a significant main effect of interference type, ($F(1, 28) = 32.247$, $p <$

.001, η^2 = 0.252, BF_{10}=2362.71). Additionally, we observed a significant effect of hand correspondence ($F(1, 28) = 5.043$, p =.033, η^2 = 0.055, BF_{10}=1.725), with no significant interaction ($F(1, 28) = 0.367$, p =.055, η^2 = 0.002, BF_{10}=0.28). The effect of hand correspondence suggested that precision was slightly lower when the hands did not correspond between the main task and the interference task ($t(28) = 2.24$, p_{holm} =.033, d = 0.276, 95% CI [0.016 0.536], BF_{10}=2.88).

Working memory gating and hand correspondence

In Hypothesis III, we predicted that shared motor features between the main and secondary tasks would trigger WM gate opening during maintenance, which should lead to an encoding of new sensory input. This will lead to an interaction between the color information already stored in WM and the task-irrelevant color of the interference task cue. Specifically, we expected this effect to manifest as an attraction bias between the interfering color and the target color in WM.

To assess whether attraction occurred, we first compared both conditions (corresponding and non-corresponding response hands) against zero using a one-tailed one sample t-test. The analysis showed that WM representations were attracted to the interfering color in both corresponding ($t(28) = 6.936$, p<.001, d = 1.288, 95% CI [2.427 ∞]; BF_{10}= 201668) and non-corresponding conditions ($t(28) = 6.077$, p<.001, d = 1.128, 95% CI [1.534 ∞]; BF_{10}= 24493).

Next, we directly compared attraction biases between corresponding and non-corresponding response hands in the visuomotor condition using a one-tailed paired-samples t-test (Figure 4A). Results indicated that when response hands corresponded between the two tasks, attraction biases were significantly higher ($t(28) = 2.580$, p=.008, d = 0.479, %95 [0.370 ∞]; BF_{10}= 6.265).

Interference task response times and accuracy

We compared the interference task RTs using a repeated measures 2x2 ANOVA (motor, visuomotor; corresponding, non-corresponding hand) to see any possible differences in the interference task performance as a function of hand correspondence (Figure 2D). Our results showed no main effect of interference type ($F(1, 28) = 2.526$, p = .123, η^2 = .03, BF_{10}=0.679) or hand correspondence ($F(1, 28) = 0.109$, p = .743, η^2 = .002, BF_{10}=0.302). While there was a significant interaction ($F(1, 28) = 5.55$, p = .026, η^2 = .032, BF_{10}=2.99), no post-hoc

comparisons reached significance (Visuomotor interference: corresponding, non-corresponding $t(28) = 1.509$, p_{holm}=.69, d = 0.072, %95 [-0.066 0.209]; Motor interference: corresponding, non-corresponding $t(28) = -0.94$, p_{holm}=1, d =-0.045, %95 [-0.181 0.120]; Corresponding hands: visuomotor, motor $t(28) = 2.654$, p_{holm}=.64, d = 0.115, %95 [-0.015 0.244]; Non-corresponding hands: visuomotor, motor $t(28) =-0.053$, p_{holm}=1, d = -0.002, %95 [-0.124 0.120]). This makes the interpretation of the interaction rather difficult.

Furthermore, we compared the proportion of correct hand use in the interference task (Figure 2C). Our 2×2 repeated measures ANOVA revealed no significant main effects (Visuomotor, motor interference: $F(1, 28) = 1.417$, $p = .244$, $\eta^2 = .006$, BF_{10}=0.355; Corresponding, non-corresponding hands: $F(1, 28) = 2.518$, $p = .124$, $\eta^2 = .058$, BF_{10}=0.928) and no significant interaction ($F(1, 28) = 0.204$, $p = .655$, $\eta^2 = .001$, BF_{10}=0.302). These results suggest that the observed difference in attraction bias between corresponding and non-corresponding conditions were not confounded by variations in task difficulty.

EEG

Contralateral mu/beta suppression

In line with Hypothesis 1, we tested whether contralateral mu suppression occurred during the encoding of visual information into WM. Results showed a significant cluster in the contralateral minus ipsilateral oscillatory activity following stimulus onset, between 180-1400ms and 6.48-30 Hz (cluster size: 4426, d_{max}=-1.244, d_{mean}=-0.726; see Figure 3A). The suppression was distributed in the mu/beta range and was localized over centroparietal regions contralateral to the responding hand in the main task, as expected. This finding suggests that motor encoding overlaps with the encoding of sensory information.

For the second part of Hypothesis 1, we also predicted that this motor preparation would be predictive of participants' behavioral accuracy, as shown in previous studies (Boettcher et al., 2021; Nasrawi et al., 2023). To test this, we split trials into high- and low-performance conditions based on each participant’s median accuracy score within each condition. Then, we compared averaged high- and low-performance trials using a cluster-based permutation test for each condition. Our results revealed no significant clusters in any condition. Thus, although the mu/beta power lateralization before the secondary task onset reflects the encoding of the response side for the later WM report, this process did not determine the accuracy of this report.

Posterior Alpha Suppression

To investigate whether the re-focusing of attention on the WM representation after an interfering task differed between the two interference conditions, we focused on differences in oscillatory activity over visual areas. We compared all conditions (motor interference, visuomotor interference, baseline) with each other, based on CBPT from the interference onset to the probe onset (1400ms – 3400ms). Results showed that posterior suppression of alpha to beta power (~8-30 Hz) was stronger in the visuomotor interference condition than the motor interference condition (between 1668-3400ms and 4-30Hz, cluster size=6550, cluster threshold=1125.5, d_{max}= -1.505, d_{mean}=-0.699; see Figure 3B). Oscillatory suppression in the motor interference condition was also higher than in the baseline condition (between 1624-2572ms and 4-27.6Hz, cluster size=2637, cluster threshold=1138.5, d_{max}=-1.170, d_{mean}=-0.576)

We further analyzed posterior oscillatory activity in a response-locked manner, focusing on oscillatory activity time-locked to the responses to the interference task. As shown in Figure 3C, a clear difference in posterior alpha activity emerged between the motor and visuomotor conditions, largely following the interfering task response (between -248-700ms and 4-30Hz,cluster size=3758, cluster threshold=666, d_{max}=-1.45, d_{mean}=-0.707). This observation suggests that the posterior alpha power differences reflect refocusing on the to-be-reported WM representation, rather than differences in processing the interference task.

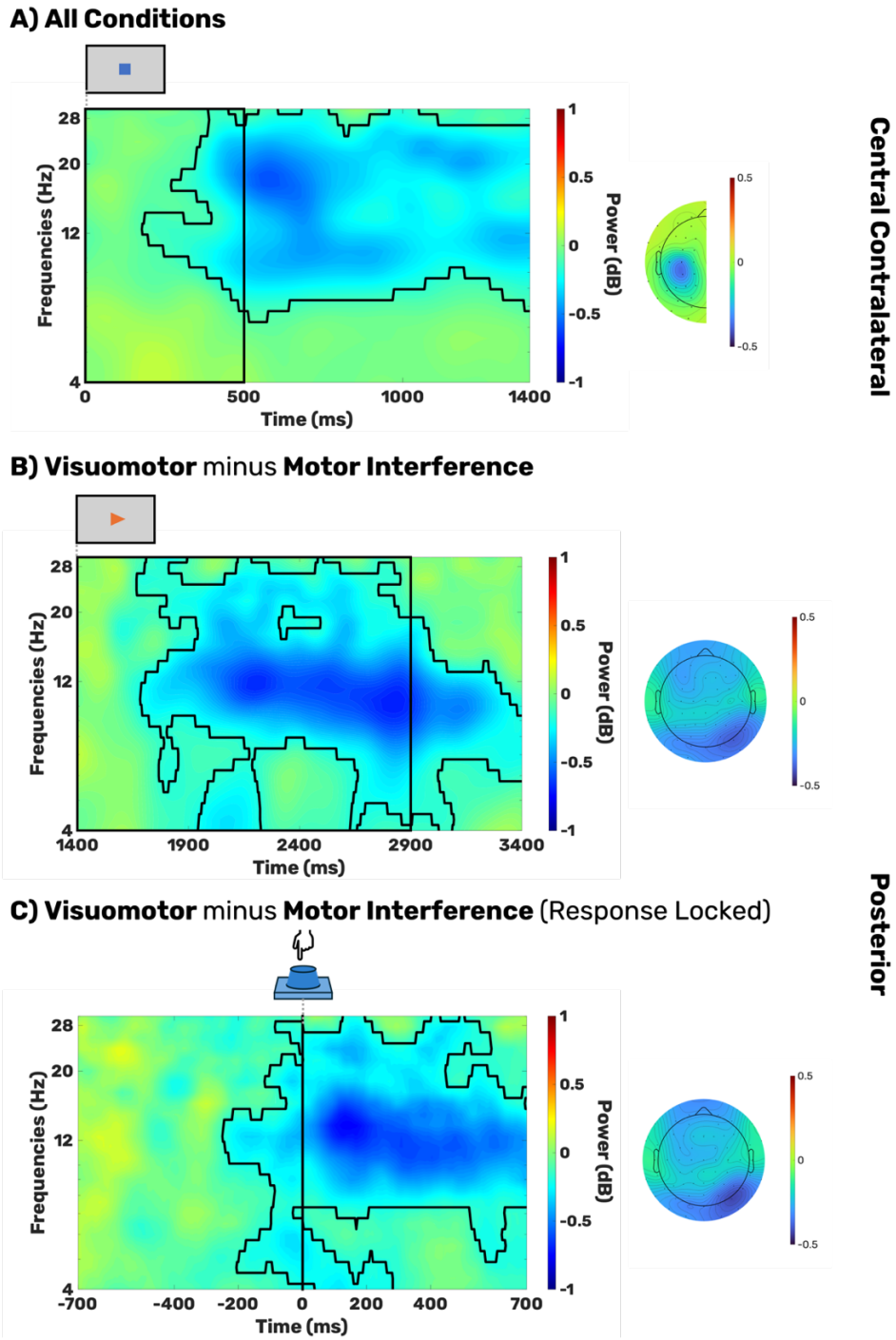

Figure 3. Early Motor Planning, and Reallocation of Attention After Interference. Black outlined areas indicate significant clusters identified through CBPT. **A)** The rectangle frame marks the target presentation window (0–500ms). Mu/beta lateralization (averaged over C3, C4, CP3, and CP4) begins early, aligning with the target's appearance on the screen. The topography reveals that this effect is localized to centro-parietal electrodes. **B)** The rectangle frame highlights the interference window (1400–2900ms). Posterior (averaged over Oz, O1, O2, Pz, PO3, and PO4) alpha/beta suppression is most pronounced in the visuomotor interference condition, suggesting greater resources allocated to refocusing on the target representation after interference. The topography shows widespread negativity across the scalp, with a stronger suppression of oscillatory power at posterior electrodes. **C)** The vertical line at 0ms shows the button press in the interference task. The posterior alpha/beta suppression difference between interference conditions emerges largely following the interference task response.

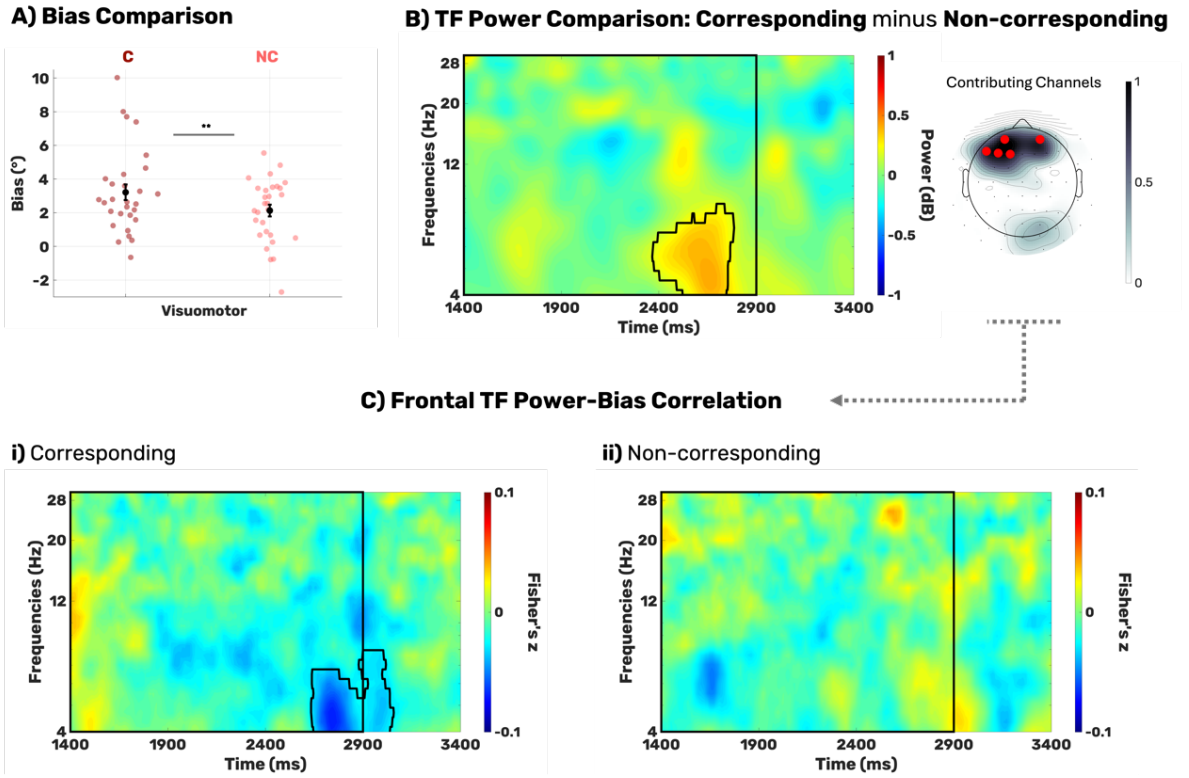

Figure 4. Response-Related Bias Effect and Frontal Theta Power. (**p*<.05, ***p*<.01, ****p*<.001) Outlined areas in the contour plots represent significant clusters identified through CBPT. Black rectangle frames represent the interference window (1400ms-2900ms) **A)** The WM representation was drawn toward the interfering color in both corresponding and non-corresponding conditions, with a stronger attraction bias in the corresponding condition. **B)** Exploratory analysis revealed increased frontal theta activity in the late phase of the interference interval in the corresponding visuomotor interference condition compared to the non-corresponding condition. The marked channels of the topography plot highlight the key contributing channels (AF3, AF4, F1, F3, and F5). **C)** In the corresponding visuomotor condition only, frontal theta activity (calculated over the contributing channels from Figure 4B) predicted the level of attraction bias on a trial-by-trial basis at the end of the interference interval. Higher theta power is associated with lower attraction bias. The time-frequency distribution of this effect closely resembled the frontal theta differences observed between conditions.

Exploratory Analysis: Frontal Theta and Bias Effect

As an exploratory analysis, we investigated potential oscillatory EEG effects linked to the attraction bias differences between the corresponding vs. non-corresponding response types in the visuomotor condition (Figure 4B). To this end, we conducted an additional CBPT across times, frequencies and channels (for details, see the Methods section). This analysis revealed a difference in theta power during the later interval between the presentation of the secondary task cue and the memory probe (between 2368-2784ms and 4-8.26Hz, t_{sum}=2094, t_{crit}=1918, d_{max}=0.75, d_{mean}=0.57). Frontal theta power was higher when the hands used in the main and the interference tasks matched in the visuomotor condition. The channels contributing most to

this effect were AF3, AF4, F1, F3, and F5 (Figure 4B). Notably, there was no evidence of differences in posterior oscillatory patterns between the corresponding and non-corresponding conditions. This suggests that the sensory information was processed similarly across these conditions, ruling out significant variations in early attentional orienting to the irrelevant color as the primary cause of the attraction bias effect.

To investigate the predictive relationship between the frontal theta difference and the attraction bias effect toward the secondary task cue color, we calculated single-trial correlations between time-frequency (TF) data and bias scores for each time point, frequency, and channel. A cluster-based permutation test was then conducted on these correlation scores, restricted to the frontal channels identified in the prior exploratory analysis. This effect was examined separately for the corresponding and non-corresponding response conditions.

Our analysis revealed that only in the visuomotor corresponding response condition did frontal theta power predict bias scores at the single-trial level (Figure 4C). Specifically, a negative relationship was observed: higher frontal theta power was associated with a lower attraction bias (between 2636-3056ms and 4-7.62Hz, cluster size=689, cluster threshold=489, dmax=-1.09, dmean=-0.61). These results suggest that the increase in frontal theta power reflects a reactive control mechanism for mitigating secondary task interference.

DISCUSSION

This study tested the role of motor processes in WM gating. Our results showed that when the planned motor responses for a WM task matched the response required for an interference task, the irrelevant visual information presented during the interference task influenced later WM report to a stronger extent. This finding suggests that motor control processes can modulate the extent to which WM is prone to irrelevant sensory information.

As shown in Figure 2A, the interference effect was linked to the presentation of irrelevant sensory information (visuomotor condition), not to a general performance decline by responding to a secondary task during WM storage (motor condition). This finding supports the notion that irrelevant visual information during maintenance can disturb visual WM representations (Lorenc et al., 2021; Rademaker et al., 2015; Saito et al., 2023), at least when this information is presented within a sensory object requiring a response.

In line with our main hypothesis, our results further revealed higher levels of attraction bias to the interfering color during visuomotor interference when the responding hand corresponded between the two tasks (see figure 4A). This finding aligns with the view that WM input gating can be influenced by actions (Chatham & Badre, 2015). According to this view, such gating adaptations may allow WM to respond dynamically to task-relevant environmental changes during action execution. This process is thought to be mediated by the basal ganglia (BG), which play a dual role in motor control (Cui et al., 2013) and sensory gating mechanisms (Slagter et al., 2012). Specifically, the Go/NoGo pathways of the basal ganglia are well-known for their role in motor control (Cui et al., 2013; Tai et al., 2012), but have also been linked to sensory updating processes in higher cortical regions (Frank et al., 2001; Frank & O'Reilly, 2006). While our study does not provide region/network-specific evidence for this mechanism, our findings conceptually align with the framework of BG-mediated WM gating mechanisms. This means that the execution of a certain motor action may open the WM gate and thus lead to the uptake of sensory information into WM. This is particularly the case when the action corresponds to motor plans already stored in WM, thereby resulting in a stronger attraction bias. However, it is also possible that the requirement of a response to the cues in the visuomotor interference task leads to an automatic transfer of the irrelevant color into WM, without the assumption of a selective gating mechanism. In this case, the response correspondence effect would not occur through the influence on WM input gating, but during the later storage of information in WM, based on a stronger attraction between two representations with overlapping motor features.

In order to break down the underlying processes in more detail, we did an exploratory analysis of the neural oscillatory patterns linked to the effect of motor correspondence in the visuomotor interference task. There was higher frontal theta power for the corresponding than for the non-corresponding visuomotor interference condition at the end of the interference task interval. This frontal theta power predicted the level of attraction bias only in the corresponding visuomotor interference condition, with higher theta power associated with a lower attraction bias (see Figure 4C). Given the role of frontal theta power in conflict resolution (Cohen & Donner, 2013; Kaiser et al., 2022; Nigbur et al., 2011; Rac-Lubashevsky & Kessler, 2015), we interpret this activity as reflecting a mechanism that actively mitigates interference arising from action-induced opening of the WM gate. The observed negative relationship in the corresponding condition suggests that the more effective this mechanism is, the weaker the attraction of the reported color to the irrelevant color from the interference task. The fact that

the relationship between theta power and subsequent WM performance is exclusively observed in the corresponding condition further demonstrates that the frontal theta power difference between the conditions (see Figure 4B) is related to the increased reliance on top-down control in the corresponding condition relative to the non-corresponding condition. This interpretation aligns with findings by Rac-Lubashevsky and Kessler (Rac-Lubashevsky & Kessler, 2015, 2018), who demonstrated that when there is an automatic tendency to update WM, but the task requires maintaining existing information, higher theta activity is observed.

Given that the motor plan interacted with the attraction effect by the visuomotor task, it must have been initiated before the interference task. In line with this, mu/beta suppression contralateral to the responding hand emerged during the presentation of the to-be-memorized object (Figure 3A). While some studies have suggested that such early correlates of motor planning prior to an interfering task can predict later WM precision (Boettcher et al., 2021; Nasrawi et al., 2023), our findings did not support this notion. However, our study did not allow participants to form precise action plans due to the randomization of the color wheel on each trial. While participants knew which hand to use, they could not anticipate the exact degree of rotation required. In contrast, Nasrawi et al. (2023) and Boettcher et al. (2021) allowed for a better prediction of the motor requirements during target report, because the starting orientation of the memory probe was fixed, enabling participants to plan the specific amount of rotation required. Additionally, our study used color as the visual WM item, whereas previous studies demonstrating this effect primarily used orientation as the target stimulus feature. Orientation may be more closely linked to motor processes than color (Huang, 2015), potentially leading to subtle differences in the mechanisms of maintenance (Kandemir et al., 2024).

Furthermore, we observed differences in posterior alpha/beta activity (~8-30 Hz) between conditions during the secondary task period (Figure 3B). Most notably, suppression of posterior alpha/beta power was stronger in the visuomotor interference condition than in the motor interference condition. This difference appeared largely after the interference task response (see Figure 3C), suggesting that it emerged after the processing of the interfering task cue was complete (i.e., when no further sensory processing of the interfering task cue was required). This timing aligns with the reorienting of attention back to the main task's WM representation. The stronger suppression of alpha/beta power after the visuomotor interference could therefore indicate greater demands for refocusing attention on the visual information stored in WM.

Conclusion

The involvement of motor processes in WM has gathered increasing attention (Boettcher et al., 2021; Nasrawi et al., 2023; Rösner et al., 2022; Schneider et al., 2017; van Ede et al., 2019; Zickerick et al., 2021). Given WM's goal-directed nature and flexibility across different contexts (Heuer et al., 2020; Huang, 2015; Özdemir et al., 2024; Trentin et al., 2023; Zhang & Yu, 2024), this focus is well-justified. In this study, we demonstrated that motor processes influence WM susceptibility to interference, with corresponding motor demands increasing attraction towards task-irrelevant information. To our knowledge, this study provides the first experimental evidence for motor processes affecting WM gating, observed at both behavioral and EEG levels. Additionally, we proposed that the uptake of irrelevant information into WM is counteracted by a reactive control mechanism reflected in frontal theta oscillatory activity, aimed at preserving the storage of task-relevant information in WM.

REFERENCES

Baddeley, A. (2003). Working memory: Looking back and looking forward. *Nature Reviews Neuroscience*, *4*(10), Article 10. https://doi.org/10.1038/nrn1201

Bergh, D. van den, Doorn, J. van, Marsman, M., Draws, T., Kesteren, E.-J. van, Derks, K., Dablander, F., Gronau, Q. F., Kucharský, Š., Gupta, A. R. K. N., Sarafoglou, A., Voelkel, J. G., Stefan, A., Ly, A., Hinne, M., Matzke, D., & Wagenmakers, E.-J. (2020). A Tutorial on Conducting and Interpreting a Bayesian ANOVA in JASP. *L'Année Psychologique*, *120*(1), 73–96. https://doi.org/10.3917/anpsy1.201.0073

Boettcher, S. E. P., Gresch, D., Nobre, A. C., & van Ede, F. (2021). Output planning at the input stage in visual working memory. *Science Advances*, *7*(13), eabe8212. https://doi.org/10.1126/sciadv.abe8212

Chatham, C. H., & Badre, D. (2015). Multiple gates on working memory. *Current Opinion in Behavioral Sciences*, *1*, 23–31. https://doi.org/10.1016/j.cobeha.2014.08.001

Chunharas, C., Rademaker, R. L., Brady, T. F., & Serences, J. T. (2022). An adaptive perspective on visual working memory distortions. *Journal of Experimental Psychology: General*, *151*(10), 2300–2323. https://doi.org/10.1037/xge0001191

Cohen, M. X., & Donner, T. H. (2013). Midfrontal conflict-related theta-band power reflects neural oscillations that predict behavior. *Journal of Neurophysiology*, *110*(12), 2752–2763. https://doi.org/10.1152/jn.00479.2013

Cui, G., Jun, S. B., Jin, X., Pham, M. D., Vogel, S. S., Lovinger, D. M., & Costa, R. M. (2013). Concurrent activation of striatal direct and indirect pathways during action initiation. *Nature*, *494*(7436), 238–242. https://doi.org/10.1038/nature11846

Delorme, A., & Makeig, S. (2004). EEGLAB: An open source toolbox for analysis of single-trial EEG dynamics including independent component analysis. *Journal of Neuroscience Methods*, *134*(1), 9–21. https://doi.org/10.1016/j.jneumeth.2003.10.009

Faul, F., Erdfelder, E., Lang, A.-G., & Buchner, A. (2007). G*Power 3: A flexible statistical power analysis program for the social, behavioral, and biomedical sciences. *Behavior Research Methods*, *39*(2), 175–191. https://doi.org/10.3758/BF03193146

Frank, M. J., Loughry, B., & O'Reilly, R. C. (2001). Interactions between frontal cortex and basal ganglia in working memory: A computational model. *Cognitive, Affective, & Behavioral Neuroscience*, *1*(2), 137–160. https://doi.org/10.3758/CABN.1.2.137

Frank, M. J., & O'Reilly, R. C. (2006). A mechanistic account of striatal dopamine function in human cognition: Psychopharmacological studies with cabergoline and haloperidol. *Behavioral Neuroscience*, *120*(3), 497–517. https://doi.org/10.1037/0735-7044.120.3.497

Günseli, E., Fahrenfort, J. J., van Moorselaar, D., Daoultzis, K. C., Meeter, M., & Olivers, C. N. L. (2019). EEG dynamics reveal a dissociation between storage and selective attention within working memory. *Scientific Reports*, *9*(1), 13499. https://doi.org/10.1038/s41598-019-49577-0

Gunseli, E., Meeter, M., & Olivers, C. N. L. (2014). Is a search template an ordinary working memory? Comparing electrophysiological markers of working memory maintenance for visual search and recognition. *Neuropsychologia*, *60*, 29–38. https://doi.org/10.1016/j.neuropsychologia.2014.05.012

Heuer, A., Ohl, S., & Rolfs, M. (2020). Memory for action: A functional view of selection in visual working memory. *Visual Cognition*, *28*(5–8), 388–400. https://doi.org/10.1080/13506285.2020.1764156

Huang, L. (2015). Color Is Processed Less Efficiently Than Orientation in Change Detection but More Efficiently in Visual Search. *Psychological Science*, *26*(5), 646–652. https://doi.org/10.1177/0956797615569577

Kaiser, J., Iliopoulos, P., Steinmassl, K., & Schütz-Bosbach, S. (2022). Preparing for Success: Neural Frontal Theta and Posterior Alpha Dynamics during Action Preparation Predict Flexible Resolution of Cognitive Conflicts. *Journal of Cognitive Neuroscience*, *34*(6), 1070–1089. https://doi.org/10.1162/jocn_a_01846

Kandemir, G., Wilhelm, S. A., Axmacher, N., & Akyürek, E. G. (2024). Maintenance of color memoranda in activity-quiescent working memory states: Evidence from impulse perturbation. *iScience*, *27*(4), 109565. https://doi.org/10.1016/j.isci.2024.109565

Lopez-Calderon, J., & Luck, S. J. (2014). ERPLAB: An open-source toolbox for the analysis of event-related potentials. *Frontiers in Human Neuroscience*, *8*. https://doi.org/10.3389/fnhum.2014.00213

Lorenc, E. S., Mallett, R., & Lewis-Peacock, J. A. (2021). Distraction in Visual Working Memory: Resistance is Not Futile. *Trends in Cognitive Sciences*, *25*(3), 228–239. https://doi.org/10.1016/j.tics.2020.12.004

Love, J., Selker, R., Marsman, M., Jamil, T., Dropmann, D., Verhagen, J., Ly, A., Gronau, Q. F., Šmíra, M., Epskamp, S., Matzke, D., Wild, A., Knight, P., Rouder, J. N., Morey, R. D., & Wagenmakers, E.-J. (2019). JASP: Graphical Statistical Software for Common Statistical Designs. *Journal of Statistical Software*, *88*, 1–17. https://doi.org/10.18637/jss.v088.i02

Miller, E. K., Lundqvist, M., & Bastos, A. M. (2018). Working Memory 2.0. *Neuron*, *100*(2), 463–475. https://doi.org/10.1016/j.neuron.2018.09.023

Nasrawi, R., Boettcher, S. E. P., & Van Ede, F. (2023). Prospection of potential actions during visual working memory starts early, is flexible, and predicts behavior. *The Journal of Neuroscience*, JN-RM-0709-23. https://doi.org/10.1523/JNEUROSCI.0709-23.2023

Nigbur, R., Ivanova, G., & Stürmer, B. (2011). Theta power as a marker for cognitive interference. *Clinical Neurophysiology*, *122*(11), 2185–2194. https://doi.org/10.1016/j.clinph.2011.03.030

Oldfield, R. C. (1971). The assessment and analysis of handedness: The Edinburgh inventory. *Neuropsychologia*, *9*(1), 97–113. https://doi.org/10.1016/0028-3932(71)90067-4

Olivers, C. N. L., & Roelfsema, P. R. (2020). Attention for action in visual working memory. *Cortex*, *131*, 179–194. https://doi.org/10.1016/j.cortex.2020.07.011

Oostenveld, R., Fries, P., Maris, E., & Schoffelen, J.-M. (2011). FieldTrip: Open Source Software for Advanced Analysis of MEG, EEG, and Invasive Electrophysiological Data. *Computational Intelligence and Neuroscience*, *2011*(1), 156869. https://doi.org/10.1155/2011/156869

Özdemir, Ş., Şentürk, Y. D., Ünver, N., Demircan, C., Olivers, C. N. L., Egner, T., & Günseli, E. (2024). Effects of Context Changes on Memory Reactivation. *Journal of Neuroscience*, *44*(36). https://doi.org/10.1523/JNEUROSCI.2096-23.2024

Pion-Tonachini, L., Kreutz-Delgado, K., & Makeig, S. (2019). ICLabel: An automated electroencephalographic independent component classifier, dataset, and website. *NeuroImage*, *198*, 181–197. https://doi.org/10.1016/j.neuroimage.2019.05.026

Postle, B. R. (2006). Working Memory as an Emergent Property of the Mind and Brain. *Neuroscience*, *139*(1), 23–38. https://doi.org/10.1016/j.neuroscience.2005.06.005

Rac-Lubashevsky, R., & Kessler, Y. (2015). Dissociating Working Memory Updating and Automatic Updating: The Reference-Back Paradigm. *Journal of Experimental Psychology Learning Memory and Cognition*, *42*. https://doi.org/10.1037/xlm0000219

Rac-Lubashevsky, R., & Kessler, Y. (2018). Oscillatory Correlates of Control over Working Memory Gating and Updating: An EEG Study Using the Reference-back Paradigm. *Journal of Cognitive Neuroscience*, *30*(12), 1870–1882. https://doi.org/10.1162/jocn_a_01326

Rademaker, R. L., Bloem, I. M., De Weerd, P., & Sack, A. T. (2015). The impact of interference on short-term memory for visual orientation. *Journal of Experimental Psychology: Human Perception and Performance*, *41*(6), 1650–1665. https://doi.org/10.1037/xhp0000110

Rösner, M., Sabo, M., Klatt, L.-I., Wascher, E., & Schneider, D. (2022). Preparing for the unknown: How working memory provides a link between perception and anticipated action. *NeuroImage*, *260*, 119466. https://doi.org/10.1016/j.neuroimage.2022.119466

Sahakian, A., Gayet, S., Paffen, C. L. E., & Van der Stigchel, S. (2025). Action consequences guide the use of visual working memory. *Journal of Experimental Psychology: Learning, Memory, and Cognition*, *51*(1), 4–13. https://doi.org/10.1037/xlm0001326

Saito, J. M., Kolisnyk, M., & Fukuda, K. (2023). Perceptual comparisons modulate memory biases induced by new visual inputs. *Psychonomic Bulletin & Review*, *30*(1), 291–302. https://doi.org/10.3758/s13423-022-02133-w

Schneider, D., Barth, A., & Wascher, E. (2017). On the contribution of motor planning to the retroactive cuing benefit in working memory: Evidence by mu and beta oscillatory activity in the EEG. *NeuroImage*, *162*, 73–85. https://doi.org/10.1016/j.neuroimage.2017.08.057

Slagter, H. A., Tomer, R., Christian, B. T., Fox, A. S., Colzato, L. S., King, C. R., Murali, D., & Davidson, R. J. (2012). PET evidence for a role for striatal dopamine in the attentional blink: Functional implications. *Journal of Cognitive Neuroscience*, *24*(9), 1932–1940. https://doi.org/10.1162/jocn_a_00255

Tai, L.-H., Lee, A. M., Benavidez, N., Bonci, A., & Wilbrecht, L. (2012). Transient stimulation of distinct subpopulations of striatal neurons mimics changes in action value. *Nature Neuroscience*, *15*(9), 1281–1289. https://doi.org/10.1038/nn.3188

Trentin, C., Falanga, L., Jeske, J., Olivers, C. N. L., & Slagter, H. A. (2024). *Action similarity warps visual feature space in working memory*. OSF. https://doi.org/10.31234/osf.io/spd78

Trentin, C., Slagter, H. A., & Olivers, C. N. L. (2023). Visual working memory representations bias attention more when they are the target of an action plan. *Cognition*, *230*, 105274. https://doi.org/10.1016/j.cognition.2022.105274

Ülkü, S., Getzmann, S., Wascher, E., & Schneider, D. (2024). Be prepared for interruptions: EEG correlates of anticipation when dealing with task interruptions and the role of aging. *Scientific Reports*, *14*(1), 5679. https://doi.org/10.1038/s41598-024-56400-y

van Ede, F. (2020). Visual working memory and action: Functional links and bi-directional influences. *Visual Cognition*, *28*(5–8), 401–413. https://doi.org/10.1080/13506285.2020.1759744

van Ede, F., Chekroud, S. R., Stokes, M. G., & Nobre, A. C. (2019). Concurrent visual and motor selection during visual working memory guided action. *Nature Neuroscience*, *22*(3), Article 3. https://doi.org/10.1038/s41593-018-0335-6

Van Ede, F., & Nobre, A. C. (2023). Turning Attention Inside Out: How Working Memory Serves Behavior. *Annual Review of Psychology*, *74*(1), 137–165. https://doi.org/10.1146/annurev-psych-021422-041757

Woodman, G. F., Wang, S., Sutterer, D. W., Reinhart, R. M. G., & Fukuda, K. (2022). Alpha suppression indexes a spotlight of visual-spatial attention that can shine on both perceptual and memory representations. *Psychonomic Bulletin & Review*, *29*(3), 681–698. https://doi.org/10.3758/s13423-021-02034-4

Zhang, M., & Yu, Q. (2024). The representation of abstract goals in working memory is supported by task-congruent neural geometry. *PLOS Biology*, *22*(12), e3002461. https://doi.org/10.1371/journal.pbio.3002461

Zickerick, B., Rösner, M., Sabo, M., & Schneider, D. (2021). How to refocus attention on working memory representations following interruptions—Evidence from frontal theta and posterior alpha oscillations. *European Journal of Neuroscience*, *54*(11), 7820–7838. https://doi.org/10.1111/ejn.15506